

<https://doi.org/10.1038/s42003-026-09718-4>

Hippocampal and cortical oscillatory dynamics support semantic processing and performance

Check for updates

Megan C. Hall¹, Maggie P. Rempe^{1,2}, Jason A. John¹, Grant M. Garrison¹, Ryan Glesinger¹, Chloe C. Casagrande¹, Nathan M. Petro¹, Hannah J. Okelberry¹, Aubrie J. Petts¹, Hua Bai¹, Seth Bashford¹, Sarah M. Dietz¹, Pamela E. May-Weeks², Brittany K. Taylor^{1,3}, Yasra Arif¹, Elizabeth Heinrichs-Graham^{1,3}, Giorgia Picci^{1,3}, Rachel K. Spooner^{1,3} & Tony W. Wilson^{1,3}✉

While extensive work has mapped the anatomical regions that support semantic processing in healthy adults, the neural dynamics of such processing remain poorly understood. Herein, we use magnetoencephalography (MEG) to assess semantic-relatedness judgements (i.e., related versus unrelated) in 150 healthy adults. MEG data were transformed into the time-frequency domain and significant task-related oscillatory responses were imaged using a beamformer. Whole-brain, voxel-wise linear mixed-effects (LME) models were used to assess conditional differences while controlling for age. We find that participants respond slower during semantically-unrelated compared to -related trials and have stronger theta oscillations during unrelated trials in bilateral inferior frontal, parietal, and hippocampal areas, with the reverse pattern in the left superior parietal. In the gamma range, participants exhibit stronger gamma oscillations during related trials in prefrontal, hippocampal, and occipital regions. These findings suggest that theta and gamma oscillations may serve distinct roles in semantic processing.

To navigate the world, the capacity to understand and conceptualize words and objects is necessary. The ability to understand visual and auditory language and connect it to concepts and environmental stimuli is often referred to as semantic processing, which is thought to occur in a distributed, left-lateralized network^{1,2}. Within the construct of semantic processing, there is semantic representation, which has frequently been conceptualized through the traditional hub and spoke model, as well as semantic control, which shares key features with the construct of cognitive control and has been operationalized through the controlled semantic cognition (CSC) framework³. Several subregions of the left prefrontal cortex (PFC) and left posterior temporal are thought to be critical to the retrieval of semantic information and semantic control more broadly in the CSC framework³. These regions are thought to support the working memory, executive function, and attentional processes that serve semantic control and retrieval, and to help constrain how activation propagates through the network supporting semantic representations³. Specifically, a distributed network of left-lateralized regions such as the ventrolateral PFC (vLPFC), left inferior frontal gyrus (IFG), angular gyrus, and the left posterior middle temporal

gyrus (pMTG) have been implicated in semantic control^{4–12}. Additionally, connectivity studies of semantic processing have found that the left IFG is highly connected with other areas of the brain, potentially reflecting its role in semantic control^{4,9,13,14}.

Most of the current literature on semantic processing has used functional MRI (fMRI), and this has resulted in a well-developed framework for the anatomic basis of semantic processing, but far less insight on the underlying neural dynamics. More temporally precise methods like electroencephalography (EEG) and magnetoencephalography (MEG) enable temporal dynamics to be parsed and are increasingly being used to investigate such neural activity. MEG/EEG research has generally shown a decrease in alpha power relative to baseline during semantic processing, as well as an increase in theta and/or gamma power^{15–18}, with the degree of spatial information widely varying between studies. For example, using a semantic matching task during MEG, Rempe and colleagues observed increased theta and gamma power bilaterally in the occipital cortex and increased theta in the left inferior frontal. However, they did not observe a difference in these neural responses between matching semantically-related

¹Institute for Human Neuroscience, Boys Town National Research Hospital, Boys Town, NE, USA. ²College of Medicine, University of Nebraska Medical Center (UNMC), Omaha, NE, USA. ³Department of Pharmacology & Neuroscience, Creighton University School of Medicine, Omaha, NE, USA.

✉ e-mail: tony.wilson@boystown.org

words and matching words based on length, which suggests these responses may reflect more basic visual and/or lexical level processing'. Regarding gamma, prior research has shown that gamma (30–70 Hz) increases when viewing high- compared to low-predictability nouns in the context of sentences, and therefore may be critical in the CSC framework¹⁹. Other work has shown that theta increases in temporal EEG electrodes when reading sentences with and without semantic violations, whereas increases in gamma activity within frontal electrodes are observed only when processing semantically correct sentences, again indicating that gamma may be important for semantic retrieval and integration²⁰. This study also showed increased gamma in parietal electrodes and increased theta coherence between left anterior and bilateral posterior electrodes during semantically-unrelated compared to -related processing, suggesting that gamma and theta may work together to modulate certain aspects of semantic processing and/or memory²⁰. Thus, overall, there is widespread agreement that theta and gamma oscillatory activity are critical for visual language processing, but the specific brain regions involved and their role in the CSC framework remains poorly understood.

The goal of the current study was to examine the neurophysiological basis of semantic processing using MEG, with a particular focus on the spatiotemporal dynamics of theta and gamma oscillations. We utilized MEG in this study to leverage the combined spatial and temporal precision, which was necessary to address our hypotheses. Further, we enrolled a large sample of healthy adults and used an established semantic processing task that required relatedness judgements to maximize our sensitivity to the

neural oscillations serving semantic control. Consistent with previous research, we expected behavioral responses to be slower to target words that were semantically-unrelated relative to -related to the preceding prime word, reflecting more extensive semantic search processes. Further, given our task design and focus on the neural dynamics, we expected robust theta and gamma oscillations across brain regions involved in semantic control, particularly subregions of the prefrontal and temporal cortices which have been broadly implicated in working memory and related processes. In agreement with some but not all previous work, we expected stronger theta oscillations during the processing of unrelated relative to related words, reflecting more demanding semantic control and search processes, and hypothesized that gamma oscillations in prefrontal cortices would be stronger during related word processing, reflecting semantic selection and integration.

Results

Behavioral analysis

Of the 163 participants, two were excluded due to low accuracy (<75% averaged across conditions), one due to technical difficulties, and 10 due to excessive artifacts in their MEG scan. The remaining 150 participants were included in the final sample ($M_{age} = 49.94$ years, $SD_{age} = 15.02$, $range_{age} = 21-87$, $N_{female} = 76$). These participants performed well on the task (see Fig. 1b), responding accurately to 96% ($SD = 4\%$) of all trials. Repeated measures ANOVAs with age as a between-subjects covariate of no interest and condition as a within-subjects factor showed a significant

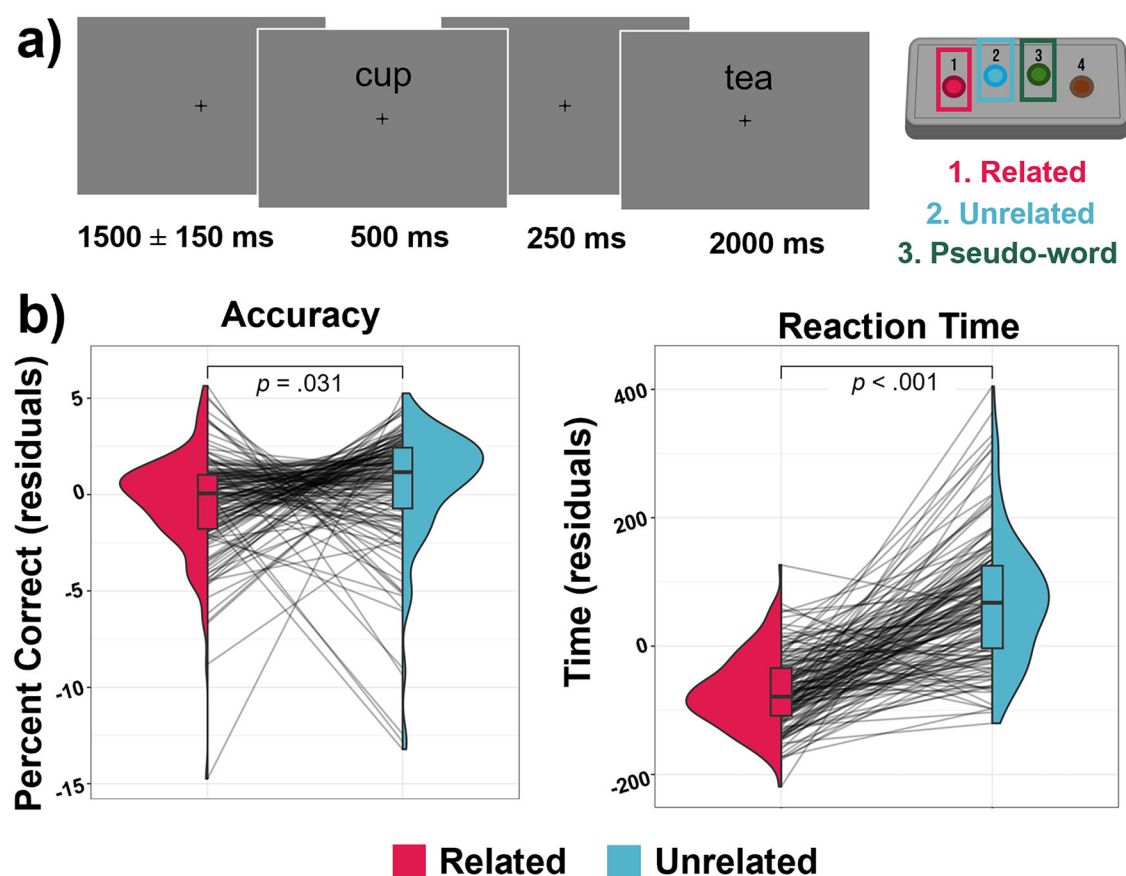


Fig. 1 | Semantic judgement paradigm and behavior. **a** Each trial started with the presentation of a central fixation cross for 1500 (± 150) ms followed by the appearance of a word above the fixation cross for 500 ms (prime), which then disappeared leaving only the fixation cross for 250 ms. Finally, a second word appeared above the fixation cross for 2000 ms (target) and participants were instructed to respond as to whether the target word was related (right index) or unrelated (right middle finger) to the prime word, or was a pseudoword (right ring

finger). The pseudowords appeared as oddballs (i.e., 10 trials) and were used to reduce mental sets; they were not included in any MEG or behavioral analyses. They were not analyzed behaviorally or neurally. **b** Accuracy (left) and reaction time (right) are shown as unstandardized residuals controlling for age. Both differed significantly between the related and unrelated conditions. Within each half-violin, the box plots show the median value with vertical lines representing values below the 25th percentile or above the 75th percentile. $N = 150$ participants.

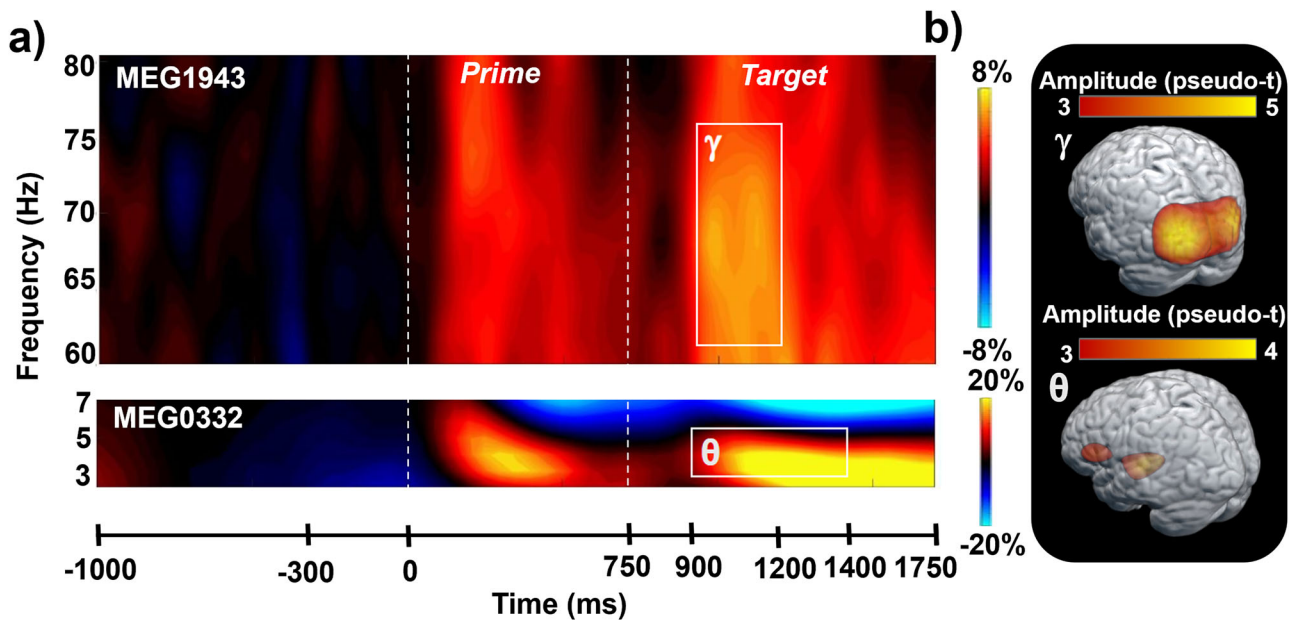


Fig. 2 | Sensor-level analysis of oscillatory strength. **a** MEG time-frequency spectrograms with time (ms) on the x-axis and frequency (Hz) on the y-axis. The onset of the prime word was 0 ms and the onset of the target word was 750 ms. Power is shown in percent change units relative to the baseline period (−1000 to −300 ms). Data has been averaged across all trials and all participants. **b** After projecting the data into source space, grand averages were computed across all participants and

conditions. There was a sustained increase in theta (3–6 Hz) in the hippocampus and left frontal cortex (bottom), while increases in gamma (62–76 Hz) were observed near the occipital cortex (top). White boxes denote the time-frequency windows used for beamforming. These time-frequency windows were statistically significant ($p < 0.001$, corrected) in the sensor level analyses. $N = 150$ participants.

difference in accuracy ($F(1, 149) = 4.77$, $p = 0.03$) and reaction time ($F(1, 149) = 228.26$, $p < 0.001$), such that participants were more accurate in the unrelated condition and responded more quickly in the related ($M = 845.20$ ms, $SD = 132.30$ ms) compared to unrelated ($M = 988.90$ ms, $SD = 187.40$ ms) condition.

Sensor-level and beamformer analysis

Statistical analysis of the sensor-level time-frequency spectrograms, irrespective of condition, revealed significant clusters of theta and gamma band oscillatory activity (Fig. 2a; $p < 0.001$). Theta band oscillatory activity increased ~150 ms after target word onset and was sustained for about 500 ms (i.e., 3–6 Hz, 900–1400 ms). Gamma band responses emerged about 200 ms following target onset and weakened about 250 ms later (i.e., 62–76 Hz, 950–1200 ms). To determine the underlying neural regions, these sensor-level time-frequency bins were imaged using a time-frequency-resolved beamformer. Note that our beamforming approach requires specific time- and frequency ranges to be specified for imaging, but these boundaries should not be interpreted as fully inclusive of the underlying oscillatory response. In general, permutation testing approaches used in EEG and MEG cannot in practice fully isolate any given neural oscillatory response. To assess data quality, the resulting whole-brain maps per neural oscillatory response were grand averaged across both conditions and all participants (Fig. 2b). This quality control analysis resulted in 135 participants being included in the analyses of theta responses and 127 being included in the analyses of gamma responses. Theta oscillations were centered in the hippocampus and left inferior frontal cortex (IFC), while gamma activity was centered in the visual cortex.

Conditional differences in oscillatory responses

To identify the neural regions sensitive to semantic relatedness, whole-brain LMEs were computed per oscillatory response identified in the sensor-level analysis. In each LME, condition was a two-level within-subjects factor and age was a continuous covariate of no interest. Neural responses in the theta range showed significant conditional differences in the bilateral inferior frontal (IFG) gyri (left: $F(1, 134) = 28.88$, $\eta^2_p = 0.18$, $p < 0.001$; right: $F(1,$

134) = 44.28, $\eta^2_p = 0.25$, $p < 0.001$), bilateral parietal (left: $F(1, 134) = 20.91$, $\eta^2_p = 0.13$, $p < 0.001$; right: $F(1, 134) = 19.04$, $\eta^2_p = 0.12$, $p < 0.001$), and right occipital ($F(1, 134) = 12.60$, $\eta^2_p = 0.09$, $p < 0.001$), such that there were stronger responses during the unrelated condition compared to the related condition (Fig. 3; $p < 0.005$, corrected). Activity in these significant clusters also extended across the right temporal cortices and the right inferior parietal ($p < 0.005$, corrected) with similar directionality. Conversely, theta oscillatory responses in the left superior parietal ($F(1, 134) = 29.00$, $\eta^2_p = 0.18$, $p < 0.001$) exhibited the opposite pattern of stronger responses during the related compared to the unrelated condition (Fig. 3; $p < 0.005$, corrected). Beyond the neocortex, significant conditional differences were detected in the bilateral hippocampi (left: $F(1, 134) = 43.61$, $\eta^2_p = 0.25$, $p < 0.001$; right: $F(1, 134) = 62.14$, $\eta^2_p = 0.21$, $p < 0.001$), with stronger theta oscillations in the unrelated compared to the related condition (Fig. 4; $p < 0.005$, corrected). In the gamma range, significant conditional differences were observed in the left IFG ($F(1, 126) = 11.55$, $\eta^2_p = 0.08$, $p < 0.001$), left cerebellum ($F(1, 126) = 16.50$, $\eta^2_p = 0.12$, $p < 0.001$), right occipital ($F(1, 126) = 12.11$, $\eta^2_p = 0.09$, $p < 0.001$), right prefrontal ($F(1, 126) = 11.07$, $\eta^2_p = 0.08$, $p = .001$), and left hippocampus ($F(1, 126) = 12.13$, $\eta^2_p = 0.09$, $p < 0.001$), such that gamma oscillations were stronger during the related compared to the unrelated condition (Fig. 5; $p < 0.005$, corrected).

Discussion

In the current study we examined the oscillatory theta and gamma dynamics underlying semantic processing, particularly in regard to semantic control operations. While many past studies have examined semantic processing using electrophysiological methods, several aspects of the current work were highly innovative. In particular, we used a whole-brain, voxel-based, beamforming approach to identify the specific brain regions exhibiting conditional task differences in neural oscillatory activity in the theta and gamma range, which is novel for this research area and provided key insight into the neural origins of the oscillatory dynamics serving semantic processing. Further, this novel aspect of the study enabled us to determine that overlapping brain regions exhibit theta and gamma task differences in the opposite direction, which is remarkable and may provide critical insight on

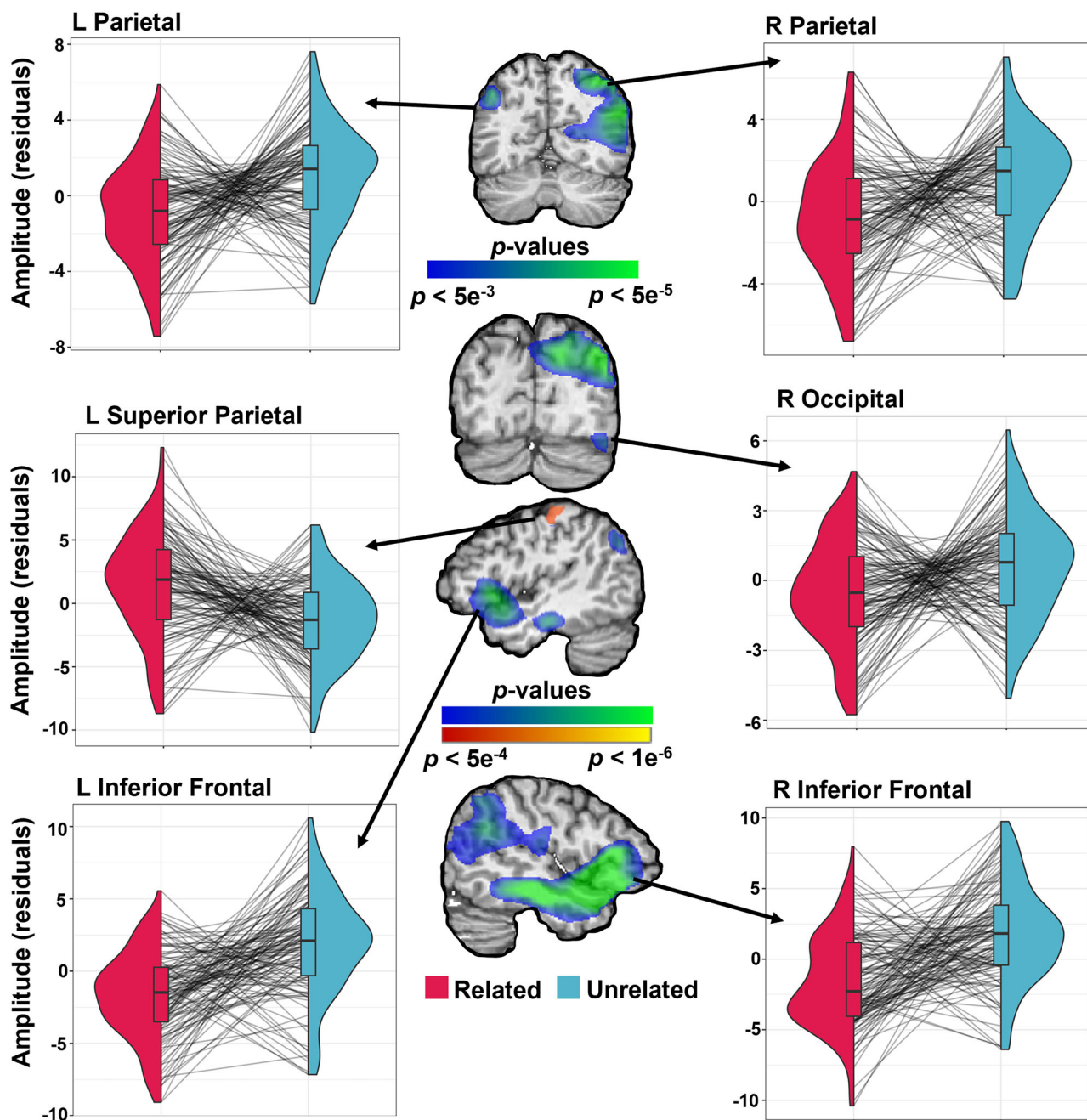


Fig. 3 | Conditional differences in theta activity. Whole-brain linear mixed-effects (LME) models controlling for age revealed significant conditional differences in theta power in the left parietal, right parietal, right occipital, and bilateral inferior frontal (IFG) gyri, such that there were stronger theta responses during the unrelated compared to the related condition (all p s < 0.005, corrected). These clusters extended along the right temporal and parietal cortices. In contrast, oscillatory responses in the left superior parietal showed the reverse pattern, with stronger theta oscillations

during the related compared to the unrelated condition. Half violin plots representing the distribution of theta amplitude for the peak voxel of each cluster (y-axis) are plotted by condition (x-axis), with lines representing individual responses in each condition. Note that unstandardized residuals are plotted on the y-axis since we controlled for age in these models. Within each half-violin, box plots show the median value of the amplitude with vertical lines representing values below the 25th percentile or above the 75th percentile. $n = 135$ participants.

the underlying neural computations. Of note, regions exhibiting such a pattern were observed in both the cortex and, critically, in the hippocampal formation. To our knowledge, no previous study of semantic processing has reported such hippocampal findings, which were robust in our study. Finally, our study included a sample size that was much larger than prior EEG and MEG studies, thus providing greater sensitivity and high experimental rigor. Regarding our specific findings, behaviorally, we found that task condition was related to reaction time and accuracy above and beyond age. Consistent with our hypothesis, participants responded significantly slower in the unrelated relative to the related condition. Conversely, they

were slightly more accurate in the unrelated compared to the related condition. While reaction time effects were expected and consistent with previous studies that focused on semantic relatedness judgements, accuracy effects were in the opposite direction from prior research, possibly due to differences in task design^{21–23}. Regarding neurophysiological activity, we found a sustained increase in theta (3–6 Hz) activity, as well as a more transient increase in gamma (62–76 Hz) activity, both of which began shortly after target onset. Our whole-brain, voxel-wise LME models revealed conditional differences in theta activity in bilateral inferior frontal regions, parietal cortices, and hippocampal areas, with stronger theta oscillations

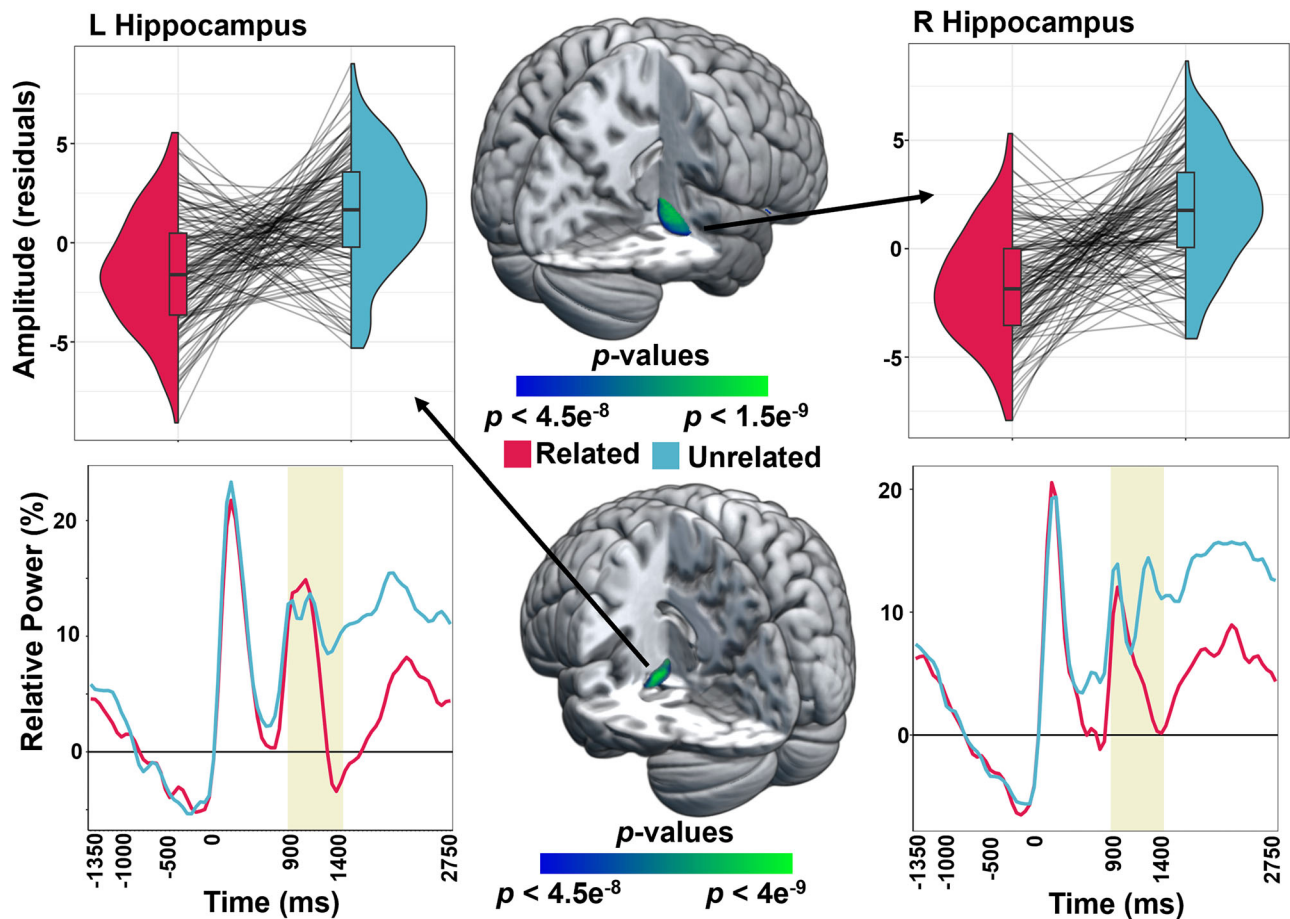


Fig. 4 | Conditional differences in theta band hippocampal activity. Whole-brain linear mixed-effects (LME) models revealed significant conditional differences in the theta band in the left and right hippocampus, such that there were stronger theta oscillations during the unrelated compared to the related condition (all $p < 0.005$, corrected). Top: Half violin plots representing the distribution of the theta response amplitude (y-axis) are plotted by condition (x-axis) for each peak, with lines representing individual responses in each condition. Since our statistical models

controlled for age, we have plotted unstandardized residuals of amplitude on the y-axis. Within each half-violin, box plots show the median value of the amplitude with vertical lines representing values below the 25th percentile or above the 75th percentile. Bottom: The relative power (percent difference from baseline; y-axis) across participants is displayed by time (x-axis) and condition (color), with the time window used to identify conditional differences (900–1400 ms) highlighted in yellow. $n = 135$ participants.

during unrelated compared to related trials. In contrast, the reverse pattern of stronger theta in related trials was observed in the left superior parietal cortex. This pattern in the left superior parietal matched our findings in the gamma range, as we found stronger gamma oscillations during related relative to unrelated trials in the left IFG, right PFC, left hippocampus, right occipital, and left cerebellum. These neural results were broadly consistent with our hypotheses, although there were some exceptions, and we did not expect the strong pattern of reversed task condition effects in theta and gamma, which is a novel finding. Below, we discuss the implications of our overall findings for understanding the role of theta and gamma oscillations in semantic processing.

As noted above, we found stronger theta oscillations in the unrelated compared to the related condition across a collection of brain regions that have been implicated in the CSC framework. These included extended areas centered on the bilateral IFG, which has been widely implicated in semantic control^{24–26}. Recent work has shown that the left IFG is specifically related to predictive processing, including the anticipation of future semantic representations, and is sensitive to semantic anomalies^{24,27}, further supporting its role in semantic control under the CSC framework³. In addition, we found stronger theta activity in the inferior parietal cortices bilaterally during the unrelated condition, which has been less commonly reported in semantic processing tasks^{28–30}. The current consensus is that these cortices may contribute to the retrieval of semantic representations and inhibition during semantic processing. We also observed significantly stronger theta

responses during unrelated trials in the right occipital cortices and the bilateral hippocampi. The hippocampal effects were somewhat surprising since this region has been more commonly reported in fMRI studies of episodic memory and because MEG is known to be less sensitive to deep brain structures. Regarding the latter, multiple MEG studies have reported neural oscillatory responses in the hippocampus and/or amygdala across a variety of cognitive tasks^{31–36}, so clearly such responses can be detected using the latest systems, at least under optimal conditions. Further, a recent study of semantic processing using MEG and the same task in a smaller sample of 33 young adults also found that theta activity in the bilateral hippocampi was stronger when viewing unrelated relative to related word pairs³⁷. Of note, these 33 participants were also included in the current study and consequently comprise about 20% of the total sample. Thus, to at least some extent, the current study could be considered a replication of this finding since ~80% of the current sample is unique. Comparing the two studies, the hippocampal results are remarkably similar, with the current study suggesting the effect is statistically very robust. Regarding the role of the hippocampal formation in semantic processing, research has historically linked the hippocampus with episodic memory and spatial navigation^{38–40}, although work focusing on semantic processing has shown hippocampal involvement in this domain as well. For example, an intracranial EEG study found correlations between hippocampal theta power and connectivity with semantic distance between recalled words⁴¹. Work from Pu et al. also found right hippocampal theta activity when participants viewed semantic

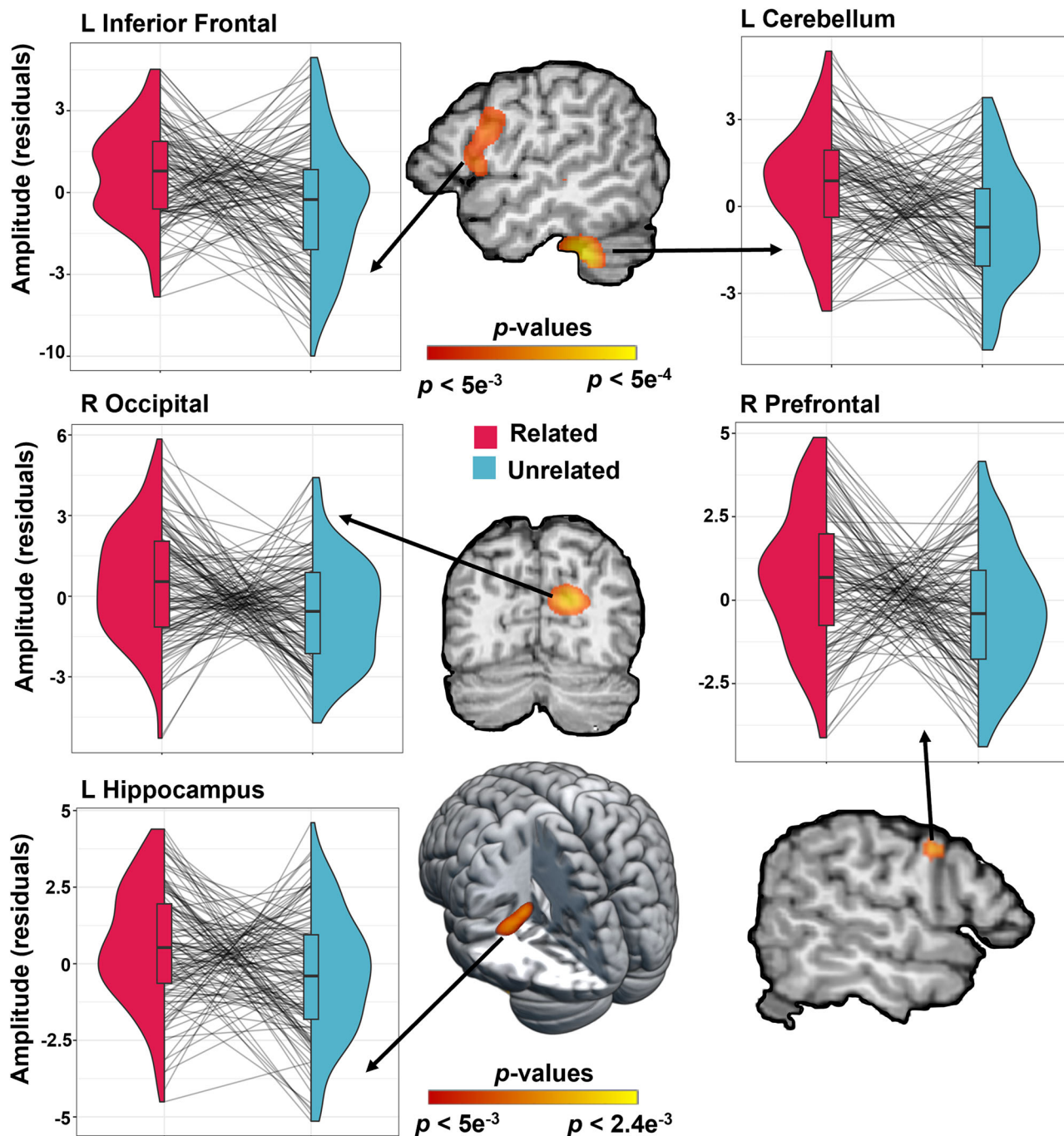


Fig. 5 | Conditional differences in gamma activity. Whole-brain linear mixed-effects (LME) models revealed significant conditional differences in the gamma band in the left inferior frontal, left cerebellum, right occipital, right prefrontal, and left hippocampus, such that there were stronger gamma oscillatory responses during the related compared to the unrelated condition (all p s < 0.005, corrected). Half violin plots representing the distribution of the amplitude (y-axis) at the peak voxel are

plotted by condition (x-axis) per cluster, with lines representing individual responses in each condition. Note again that we have plotted unstandardized residuals of amplitude on the y-axis since we controlled for age in these models. Within each half-violin, box plots show the median value of the amplitude with vertical lines representing values below the 25th percentile or above the 75th percentile. $n = 127$ participants.

violations relative to correct sentences. This and additional research in fMRI builds on O’Keefe’s original theory that the left hippocampus is involved in maintaining, updating, and retrieving information on semantic information, also called semantic mapping^{42–44}. Altogether, the current findings support prior research which has implicated hippocampal theta activity in semantic memory retrieval, especially in the context of semantic anomalies, with an important role for each of these regions in CSC³. Finally, we observed the opposite pattern of stronger theta in the related relative to the unrelated condition in the left superior parietal. Prior research has

connected theta activity in the parietal cortices to selective attention^{45,46}, although its particular role in judgments of semantic relatedness is less clear and should be further examined in future work.

In stark contrast to the theta findings, all of our gamma results indicated stronger gamma oscillations during semantically-related trials relative to -unrelated trials. Similar to the theta band, we found responses in the left IFG, further implicating this region in semantic prediction under the CSC framework^{3,19,24,27}, as well as occipital cortices and the left hippocampus. Although gamma activity in the hippocampus has previously been most

strongly associated with episodic memory^{47,48}, the current findings support an additional role for gamma hippocampal activity in semantic retrieval. However, caution is warranted given the reduced sensitivity of MEG to deeper sources of neural activity such as the hippocampus. While we offset this concern by minimizing the ambient environment noise levels through a two-layer shielded room and use of the latest MEG sensor technology, and maximizing the signal strength through task design and including a high number of artifact free epochs, this brain region still remains a challenge for detection with MEG, although several recent works have provided strong evidence supporting MEG's ability to detect such activity^{33,37}. Regarding the occipital responses, gamma oscillations in this area have been broadly implicated in visual processing, attentional control, and visual information integration⁴⁹⁻⁵¹. In contrast, prior research has mostly implicated prefrontal gamma in conflict monitoring and working memory, thus the right prefrontal gamma activity we observed here could reflect semantic control processes^{52,53}. Finally, unlike theta, we found gamma differences in cerebellar cortices. While prior research has focused on the cerebellum as a motor hub, cerebellar gamma power has also been implicated in cognitive interference and flexibility⁵⁴⁻⁵⁶ and thus along with the prefrontal region, may reflect the semantic control aspect of semantic processing. Altogether, these results indicate that both gamma and theta may be necessary for higher order control functions that are vital for semantic processing, in line with the CSC framework³. Interestingly, prior work using MEG and the same task did not find conditional differences in the gamma range³⁷. Thus, these gamma findings are novel and their relationship with theta may suggest a key computational role.

One of the most interesting and novel aspects of this study is that the theta and gamma findings were in the opposite direction. Specifically, across all significant clusters except the left superior parietal, theta activity was stronger in the unrelated condition while gamma oscillations were stronger in the related condition. In one of the first studies to examine semantic violations in online sentence processing, similar directionality was observed with theta increasing more strongly in incongruent trials whereas gamma increased more strongly in congruent trials⁵⁷. Hald et al. interpreted their findings as showing that theta is recruited for semantic retrieval and verbal working memory processes that are necessary for semantic tasks and may also serve a role in error detection. On the other hand, gamma power was tentatively interpreted as being required for normal language processing, and to be suppressed when semantic violations were present⁵⁷. While few studies since have reported both gamma and theta power in a semantic relatedness task, Mellem et al. did report marginally greater anterior-posterior theta coherence in the unrelated condition with much stronger gamma in the related condition during a semantic judgment task. While they did not further explore theta conditional differences, stronger gamma in the related condition was similarly interpreted as being associated with basic semantic processing and semantic unification²⁰. Further, recent studies reporting theta or gamma responses support this directionality for both theta^{37,58} and gamma^{19,59} during semantic tasks. For instance, Rempe et al. showed similar hippocampal effects in the theta band, but they did not report gamma band effects. Thus, despite the broad support for frequency-specific effects in the theta and gamma range during semantic processing in prior literature, the current study uniquely shows both bands working in unison with opposite directionality. The current study also broadly expands on the findings of Hald et al., by moving from scalp electrode-based measures of neural activity to identifying neuronal origins of the oscillatory signatures using a much larger sample size. These differences in study design enabled us to detect a widespread network of regions showing conditional effects with opposite directionality in the theta and gamma bands. Altogether, the results of the current study lend additional support to the role of theta and gamma in semantic control, but importantly also provides perhaps the clearest indication that these oscillatory responses have different functional roles, respond in opposite directions to semantic manipulations, and are vital for supporting semantic control and processing under the CSC framework³.

While this study contributes substantially to our understanding of the neurophysiology underlying semantic processing, it is not without limitations. First, we used a single semantic processing task and focused on the visual modality. Future work could examine different tasks and/or different presentation modalities to decipher whether the regions reported here reflect modality-specific semantic control areas or are more poly-modal and serve semantics regardless of the input modality. Second, as noted above, MEG is less sensitive to deep sources and thus our hippocampal findings should be interpreted with caution. However, it should be noted that we used the latest MEG technology, and these recordings were performed in a magnetically silent environment, with very few sources of interference. Further, much of our experimental design and analysis methods followed recommendations from Ruzich et al., including a trial design which maximized reliable contrast and timing of hippocampal activation, precise MRI coregistration, and the use of beamformer-based source estimates. Thus, conditions were optimal for detecting such deep sources and support multiple recent studies that have reported hippocampal sources and/or other deep structures^{33,34,37,60}. One recommendation we did not follow was using a physiologically constrained hippocampal model; as we were not expecting hippocampal activity, we utilized a whole-brain analytic approach instead, and future research should examine task-based activity with a more precise model⁶⁰. Third, we also focused on healthy adults who spoke English as their primary language and thus our results may not generalize to youth or individuals who speak other languages. Future work in these areas is necessary. Fourth, none of our significant clusters showed peaks in the left anterior temporal lobe, which prevented us from robustly examining relationships among regions involved in semantic control versus semantic representation. Thus, this should be a goal of future work. Finally, we did not examine dynamic functional connectivity, as we did not have specific hypotheses, but studies should consider this direction, as it would help inform on the precise role of the hippocampus and perhaps the opposing effects we observed in theta and gamma ranges.

In conclusion, the current study used advanced dynamic MEG imaging in a large sample of healthy adults to quantify neural oscillatory activity during semantic processing and elucidate the specific roles of theta and gamma oscillations. Our results indicated that theta oscillations are stronger during unrelated trials, where semantic search and control processes are more extensive, while gamma oscillations are stronger in related trials, where search processes are putatively more spatially constrained. This was true across a collection of language related brain regions in both the left and right frontal, parietal, and temporal cortices. These findings extend prior research and provide new insights into the neurophysiology underlying semantic control, with implications for oscillatory coding of semantic operations in the healthy brain.

Methods

Participants

One-hundred and sixty-three healthy adult participants were included in this study ($M_{\text{age}} = 49.64$ years, $SD_{\text{age}} = 15.12$, $\text{range}_{\text{age}} = 21-87$ years, $N_{\text{female}} = 82$). Note that this sample is an extension of that in Rempe et al. and all 33 participants in their final sample were included in the current study. Initial exclusionary criteria included any medical illness affecting CNS function, neurological or psychiatric disorder, history of head trauma, current substance misuse, and presence of any type of ferromagnetic implanted material that could interfere with the MEG or be an MRI safety concern. The study protocol was approved by the Boys Town National Research Hospital Institutional Review Board. Written informed consent was obtained from all participants after a full description of the study was provided. All ethical regulations relevant to human research participants were followed.

Experimental paradigm

Participants performed a validated semantic judgement task during MEG recording (Fig. 1a;³⁷). Each trial began with the presentation of a central

fixation crosshair for 1500 ms (± 150 ms). Then, a word (prime) appeared above the fixation cross for 500 ms. The prime then disappeared and only the fixation crosshair remained for another 250 ms. Finally, a second (target) word appeared in the same location as the prime for 2000 ms. Participants were instructed to fixate on the crosshair and respond based on whether the target word was related semantically to the prime with their right index finger (“related”), semantically-unrelated with their right middle finger (“unrelated”), or a pseudo-word with their right ring finger (“pseudoword”). Related, unrelated, and pseudoword conditions were presented to each participant in a pseudorandomized order to control for order effects. All words were 3–4 letters in length to prevent excessive eye movement. The related and unrelated words were derived from the Semantic Priming Project word list⁶¹ and were balanced for length, frequency of use, part of speech, bigram frequency, and number of orthographic neighbors. We also balanced across conditions on word concreteness, which based on data from ref. 62. Words that could elicit strong emotions in some participants or require above-average education level were excluded. All participants completed a brief practice session of the task prior to MEG recording to ensure adherence to task instructions. Each trial lasted 4250 ms (± 150 ms) and there was a total of 210 trials (i.e., 100 related, 100 unrelated, and 10 pseudoword), resulting in a total runtime of ~ 14.88 min. Pseudoword trials were included to minimize mental sets and promote cognitive flexibility. They were not included in the behavioral or neural analysis, including in the definition of our time-frequency windows.

MEG data acquisition

Participants were seated in a non-magnetic chair within a VACOSHIELD magnetically-shielded room (Vacuumschmelze, Hanau, Germany). A MEGIN Neo MEG system (Helsinki, Finland), equipped with 306 sensors including 204 planar gradiometers and 102 magnetometers, was used to sample neuromagnetic responses continuously at 1 kHz with an acquisition bandwidth of 0.1–330 Hz. Participants were monitored by a real-time audio-video feed from inside the shielded room throughout MEG data acquisition. Data from each participant were individually corrected for head movement and noise reduced using a signal space separation method with a temporal extension (tSSS)⁶³.

Structural MRI and MEG coregistration

Before MEG recording, five coils were attached to the participant’s head and localized, together with the three fiducial locations (i.e., nasion, left and right preauriculars) and scalp surface points, using a 3D digitizer (Fastrak; Polhemus Navigator Sciences, Colchester, VT). Once the participant was positioned for MEG recording, an electric current with a unique frequency label (e.g., 322 Hz) was fed to each of the five coils. This induced a measurable magnetic field and allowed each coil to be localized in reference to the sensors throughout the recording session. Head motion correction leveraged the temporal precision of MEG by estimating the location of each coil in 10 ms steps over 200 ms windows and spatially transforming the data back to the original head position (i.e., the location of the head when the recording was started). Of note, this procedure differs from the standard approaches used in fMRI and other fields, as the amount of motion (or framewise displacement) is not regressed out, but instead the actual location of the head is transformed to the correct location per time window. Across the sample, the mean max drift per time slice was 0.59 mm ($SD = 0.61$ mm) and the mean total drift across the full recording was 6.55 mm ($SD = 6.82$). Such correction is consistent with Good Practice guidelines^{63,64}. Since coil locations were also known in head coordinates, all MEG measurements could be transformed into a common coordinate system. With this coordinate system, each participant’s MEG data were co-registered with their structural T1-weighted MRI data prior to source space analyses using BESA MRI (Version 3.0; BESA GmbH, Gräfelting, Germany). All structural MRI data were acquired on a 3 T Siemens Prisma magnet using a 32-channel head coil with the following parameters: TR: 2400 ms; TE: 2.05 ms; field of view: 256 mm; matrix: 256 \times 256; slice thickness: 1 mm with no gap; voxel size: 1.0 \times 1.0 \times 1.0 mm; acquisition plane: sagittal; flip angle: 8 degrees. These

anatomical images were aligned parallel to the anterior and posterior commissures and transformed into standardized space. Following source analysis (i.e., beamforming), each participant’s functional MEG images were also transformed into standardized space using the transform that was previously applied to the structural MRI volume and spatially resampled.

MEG time-frequency transformation and statistics

MEG preprocessing and imaging was completed using the Brain Electrical Source Analysis (BESA V7.1) software. Cardiac and eye-blink artifacts were manually removed from the MEG data prior to statistical analysis using signal-space projection (SSP⁶⁵), which was accounted for during source reconstruction. The continuous magnetic time series was divided into epochs of 4100 ms duration with the prime word onset being 0 ms, target word presentation occurring at 750 ms, and the baseline period being defined as -1000 to -300 ms prior to onset of the prime. Epochs containing artifacts were rejected based on individual amplitude and gradient thresholds. The average amplitude threshold was 1167.34 ($SD = 342.29$) fT/cm and the average gradient threshold was 420.34 ($SD = 199.56$) fT/(cm*ms) across all participants and conditions. Only trials where participants responded correctly were used for analysis. On average, 86.93 ($SD = 5.61$) related and 87.32 ($SD = 6.39$) unrelated trials remained after artifact rejection and were used in subsequent analyses. Importantly, the number of trials did not significantly differ between the related and unrelated conditions ($p = 0.391$).

Artifact-free epochs were transformed into the time-frequency domain using complex demodulation⁶⁶ with a resolution of 1 Hz and 50 ms for frequencies from 2 to 30 Hz, and a resolution of 2 Hz and 25 ms for frequencies from 60 to 90 Hz. The resulting spectral power estimations per sensor were averaged across all artifact-free trials, regardless of condition, to generate time-frequency plots of mean spectral density. These sensor-level data were normalized per time-frequency bin using the respective bin’s baseline power, which was calculated as the mean power during the -1000 ms to -300 ms time period.

The specific time-frequency windows used for imaging were determined by cluster-based permutation testing of the sensor-level spectrograms across all participants and trials, restricted to the entire array of gradiometers and the theta (3–7 Hz) and gamma (30–90 Hz) ranges. To reduce the risk of false positive results while maintaining reasonable sensitivity, a two-stage procedure was followed to control for Type I error. In the first stage, paired-samples t tests against baseline were conducted on each data point and the output spectrogram of t values was thresholded at $p < 0.05$ to identify time-frequency bins containing potentially significant oscillatory deviations relative to baseline across all participants and conditions. In the second stage, time-frequency bins that survived the threshold were clustered with temporally, spectrally, and/or spatially neighboring bins with t values that were also above the ($p < 0.05$) threshold, and a cluster value was derived by summing all the t values of all data points in the cluster. Non-parametric permutation testing was then used to derive a distribution of cluster-values, and the significance level of the observed clusters (from stage one) were tested directly using this distribution^{67,68}. For each comparison, 10,000 permutations were computed to build a distribution of cluster values. Based on these analyses, only the time-frequency windows that contained significant oscillatory events ($p < 0.001$) across all trials were subjected to source imaging. Herein, we focused on the theta (3–6 Hz) and gamma (62–76 Hz) bands from 900 to 1400 ms and 950 to 1200 ms, respectively, because these time-frequency windows were significant following permutation testing and contained the strongest responses relative to baseline. Note that our beamforming approach requires specific time- and frequency ranges to be specified for imaging (see Section “Sensor-level and beamformer analysis”); however, we are aware that the windows identified through permutation testing do not necessarily contain isolated neural oscillatory responses⁶⁹, and the obtained clusters may be slightly different temporally and spatially from the underlying response. Source images were computed for each of these two time-frequency windows per condition and participant and these were used to test our hypothesized effects.

MEG source imaging and statistics

Cortical responses were source imaged using dynamic imaging of coherent sources (DICS⁷⁰), a time-frequency-resolved extension of the linearly constrained minimum variance (LCMV) beamformer⁷¹, which applies spatial filters to time-frequency sensor data to calculate voxel-wise source power for the entire brain volume. The single images are derived from the cross spectral densities of all combinations of MEG gradiometers averaged over the time-frequency range of interest, and the solution of the forward problem for each location on a grid specified by input voxel space. Following convention, we computed noise-normalized, source power per voxel in each participant using active (i.e., task) and passive (i.e., baseline) periods of equal duration and bandwidth⁷². Such images are typically referred to as pseudo-t maps and in this study were computed per participant at $4.0 \times 4.0 \times 4.0$ mm resolution using the statistically determined time-frequency windows (see above). The resulting 3D maps of brain activity were averaged across all participants and both conditions to assess data quality and for initial visualization of brain regions contributing to each significant oscillatory responses identified through the sensor-level analysis. Based on this quality control analysis, a sample of 135 participants for theta responses and 127 participants for gamma responses were included in the final statistical analyses. For a more comprehensive description of our MEG analysis and imaging methods, see Wiesman and Wilson⁷³.

Statistics and reproducibility

For behavioral analyses, we computed repeated measures ANOVAs using the *nlme()* package in R (v4.2.0) with reaction time and accuracy as dependent variables using the following formula: $\text{behavior} \sim \text{condition} + \text{age}$, $\text{random} = \sim 1 | \text{subID}$ ^{74,75}. In these models, age was a between-subjects covariate of no interest and condition (i.e., related vs unrelated) was a two-level within-subjects factor. *nlme()* was also utilized to create unstandardized residuals controlling for age for the purposes of consistency in visualization with the following formula: $\text{peak_response} \sim \text{age}$, $\text{random} = \sim 1 | \text{subID}$.

To identify the brain regions serving semantic processing, whole-brain linear mixed-effects (LME) models were calculated for each significant oscillatory response separately to examine the main effect of task condition (fixed factor with 2 levels; i.e., semantically-related and -unrelated) while controlling for age (continuous fixed factor) using custom functions in MATLAB. Participant ID was included as a random factor. On the resulting images, we employed a stringent alpha threshold of $p < 0.005$ and cluster-size threshold of $k > 4$ voxels (i.e., 256 mm^3), although the peak voxels in the conditional difference maps often far exceeded this $p < 0.005$ threshold and the significant clusters were generally much larger than four voxels. Of note, this cluster approach controls the rate of false positives across the whole-brain volume based on the theory of Gaussian random fields^{76,77} and were applied per whole-brain map (i.e., for theta and gamma separately). Notably, because condition is our only within-subjects factor and has only one observation per condition and subject, our analysis meets criteria for only using a random intercept (without random slopes)⁷⁸.

Reporting summary

Further information on research design is available in the Nature Portfolio Reporting Summary linked to this article.

Data availability

All data are publicly available via the Collaborative Informatics and Neuroimaging Suite (COINS; <https://coins.trendscenter.org/>) upon request.

Code availability

The MEG and MRI analyses reported herein utilized the Brain Electrical Source Analysis software (BESA Research: version 7.1; BESA MRI: version 3.0; BESA Statistics: version 2.1). We also used RStudio version 4.2.0 for statistical analyses. Any requests for code or batch functions used in these analyses are available upon request.

Received: 30 September 2025; Accepted: 5 February 2026;

Published online: 17 February 2026

References

1. Rempe, M. P. et al. Alpha oscillations in left perisylvian cortices support semantic processing and predict performance. *Cereb. Cortex* **32**, 5376–5387 (2022).
2. Thompson-Schill, S. L., D'Esposito, M., Aguirre, G. K. & Farah, M. J. Role of left inferior prefrontal cortex in retrieval of semantic knowledge. A reevaluation. *Proc. Natl. Acad. Sci.* **94**, 14792–14797 (1997).
3. Lambon Ralph, M. A., Jefferies, E., Patterson, K. & Rogers, T. T. The neural and computational bases of semantic cognition. *Nat. Rev. Neurosci.* **18**, 42–55 (2017).
4. Binney, R. J. et al. The ventral and inferolateral aspects of the anterior temporal lobe are crucial in semantic memory: evidence from a novel direct comparison of distortion-corrected fMRI, rTMS, and semantic dementia. *Cereb. Cortex* **20**, 2728–2738 (2010).
5. Davey, J. et al. Automatic and controlled semantic retrieval: TMS reveals distinct contributions of posterior middle temporal gyrus and angular gyrus. *J. Neurosci.* **35**, 15230–15239 (2015).
6. Hoffman, P., Jefferies, E. & Lambon Ralph, M. A. Ventrolateral prefrontal cortex plays an executive regulation role in comprehension of abstract words: convergent neuropsychological and repetitive TMS evidence. *J. Neurosci.* **30**, 15450–15456 (2010).
7. Hoffman, P., Binney, R. J. & Lambon Ralph, M. A. Differing contributions of inferior prefrontal and anterior temporal cortex to concrete and abstract conceptual knowledge. *Cortex* **63**, 250–266 (2015).
8. Jefferies, E. The neural basis of semantic cognition: converging evidence from neuropsychology, neuroimaging and TMS. *Cortex* **49**, 611–625 (2013).
9. McDonald, C. R. et al. Multimodal imaging of repetition priming: using fMRI, MEG, and intracranial EEG to reveal spatiotemporal profiles of word processing. *NeuroImage* **53**, 707–717 (2010).
10. Mollo, G., Jefferies, E., Cornelissen, P. & Gennari, S. P. Context-dependent lexical ambiguity resolution: MEG evidence for the time-course of activity in left inferior frontal gyrus and posterior middle temporal gyrus. *Brain Lang.* **177–178**, 23–36 (2018).
11. Noonan, K. A., Jefferies, E., Corbett, F. & Lambon Ralph, M. A. Elucidating the nature of deregulated semantic cognition in semantic aphasia: evidence for the roles of prefrontal and temporo-parietal cortices. *J. Cogn. Neurosci.* **22**, 1597–1613 (2010).
12. Noonan, K. A., Jefferies, E., Visser, M. & Lambon Ralph, M. A. Going beyond inferior prefrontal involvement in semantic control: evidence for the additional contribution of dorsal angular gyrus and posterior middle temporal cortex. *J. Cogn. Neurosci.* **25**, 1824–1850 (2013).
13. Binney, R. J., Parker, G. J. M. & Lambon Ralph, M. A. Convergent connectivity and graded specialization in the rostral human temporal lobe as revealed by diffusion-weighted imaging probabilistic tractography. *J. Cogn. Neurosci.* **24**, 1998–2014 (2012).
14. Davey, J. et al. Exploring the role of the posterior middle temporal gyrus in semantic cognition: integration of anterior temporal lobe with executive processes. *NeuroImage* **137**, 165–177 (2016).
15. Klimesch, W., Schimke, H. & Schwaiger, J. Episodic and semantic memory: an analysis in the EEG theta and alpha band. *Electroencephalogr. Clin. Neurophysiol.* **91**, 428–441 (1994).
16. Klimesch, W., Doppelmayr, M., Pachinger, T. & Russegger, H. Event-related desynchronization in the alpha band and the processing of semantic information. *Cogn. Brain Res.* **6**, 83–94 (1997).
17. Maguire, M. J., Brier, M. R. & Ferree, T. C. EEG theta and alpha responses reveal qualitative differences in processing taxonomic versus thematic semantic relationships. *Brain Lang.* **114**, 16–25 (2010).

18. Röhm, D., Klimesch, W., Haider, H. & Doppelmayr, M. The role of theta and alpha oscillations for language comprehension in the human electroencephalogram. *Neurosci. Lett.* **310**, 137–140 (2001).
19. Mamashli, F., Khan, S., Obleser, J., Friederici, A. D. & Maess, B. Oscillatory dynamics of cortical functional connections in semantic prediction. *Hum. Brain Mapp.* **40**, 1856–1866 (2019).
20. Mellem, M. S., Friedman, R. B. & Medvedev, A. V. Gamma- and theta-band synchronization during semantic priming reflect local and long-range lexical–semantic networks. *Brain Lang.* **127**, 440–451 (2013).
21. Frishkoff, G. A. Hemispheric differences in strong versus weak semantic priming: Evidence from event-related brain potentials. *Brain Lang.* **100**, 23–43 (2007).
22. Rissman, J., Eliassen, J. C. & Blumstein, S. E. An event-related fMRI investigation of implicit semantic priming. *J. Cogn. Neurosci.* **15**, 1160–1175 (2003).
23. Tiedt, H. O., Ehlen, F. & Klostermann, F. Age-related dissociation of N400 effect and lexical priming. *Sci. Rep.* **10**, 20291 (2020).
24. He, Y. et al. Diverse frontoparietal connectivity supports semantic prediction and integration in sentence comprehension. *J. Neurosci.* **45**, e1404242024 (2025).
25. Jackson, R. L. The neural correlates of semantic control revisited. *NeuroImage* **224**, 117444 (2021).
26. Wawrzyniak, M. et al. Fronto-temporal interactions are functionally relevant for semantic control in language processing. *PLOS ONE* **12**, e0177753 (2017).
27. Caucheteux, C., Gramfort, A. & King, J.-R. Evidence of a predictive coding hierarchy in the human brain listening to speech. *Nat. Hum. Behav.* **7**, 430–441 (2023).
28. Lam, N. H. L., Schoffelen, J.-M., Uddén, J., Hultén, A. & Hagoort, P. Neural activity during sentence processing as reflected in theta, alpha, beta, and gamma oscillations. *NeuroImage* **142**, 43–54 (2016).
29. Lydon, E. A. et al. EEG theta and alpha oscillations in early versus late mild cognitive impairment during a semantic Go/NoGo task. *Behav. Brain Res.* **416**, 113539 (2022).
30. Salisbury, D. F. & Taylor, G. Semantic priming increases left hemisphere theta power and intertrial phase synchrony. *Psychophysiology* **49**, 305–311 (2012).
31. Badura-Brack, A. S. et al. Resting-state neurophysiological abnormalities in posttraumatic stress disorder: a magnetoencephalography study. *Front. Hum. Neurosci.* **11**, 205 (2017).
32. McDermott, T. J. et al. Male veterans with PTSD exhibit aberrant neural dynamics during working memory processing: an MEG study. *J. Psychiatry Neurosci.* **41**, 251–260 (2016).
33. Meehan, C. E. et al. Differences in rhythmic neural activity supporting the temporal and spatial cueing of attention. *Cereb. Cortex* **31**, 4933–4944 (2021).
34. Petro, N. M. et al. Oscillatory brain dynamics underlying affective face processing. *Soc. Cogn. Affect. Neurosci.* **20**, nsaf047 (2025).
35. Proskovec, A. L., Heinrichs-Graham, E. & Wilson, T. W. Aging modulates the oscillatory dynamics underlying successful working memory encoding and maintenance. *Hum. Brain Mapp.* **37**, 2348–2361 (2016).
36. Wilson, T. W. et al. Aberrant neuronal dynamics during working memory operations in the aging HIV-infected brain. *Sci. Rep.* **7**, 41568 (2017).
37. Rempe, M. P. et al. Hippocampal and cortical oscillatory dynamics reflect semantic processing and predict behavioural performance. *J. Physiol.* **603**, 3089–3106 (2025).
38. Aghajyan, S. L. et al. Associations between episodic memory and hippocampal volume in late adulthood. *Hippocampus* **35**, e70010 (2025).
39. Gorbach, T. et al. Longitudinal association between hippocampus atrophy and episodic-memory decline. *Neurobiol. Aging* **51**, 167–176 (2017).
40. Snytte, J. et al. Structure–function interactions in the hippocampus and prefrontal cortex are associated with episodic memory in healthy aging. *eNeuro* **11**, ENEURO.0418-23 (2024).
41. Solomon, E. A., Lega, B. C., Sperling, M. R. & Kahana, M. J. Hippocampal theta codes for distances in semantic and temporal spaces. *Proc. Natl. Acad. Sci.* **116**, 24343–24352 (2019).
42. Pu, Y., Cheyne, D., Sun, Y. & Johnson, B. W. Theta oscillations support the interface between language and memory. *NeuroImage* **215**, 116782 (2020).
43. O’Keefe, J. & Nadel, L. *The Hippocampus as a Cognitive Map* (Oxford University Press, 1978).
44. Zheng, X. Y. et al. Parallel cognitive maps for multiple knowledge structures in the hippocampal formation. *Cereb. Cortex* **34**, bhad485 (2024).
45. Fellrath, J., Mottaz, A., Schnider, A., Guggisberg, A. G. & Ptak, R. Theta-band functional connectivity in the dorsal fronto-parietal network predicts goal-directed attention. *Neuropsychologia* **92**, 20–30 (2016).
46. Son, J. J. et al. Oscillatory dynamics serving visual selective attention during a Simon task. *Brain Commun.* **5**, fcad131 (2023).
47. Griffiths, B. J., Martin-Buro, M. C., Staresina, B. P. & Hanslmayr, S. Disentangling neocortical alpha/beta and hippocampal theta/gamma oscillations in human episodic memory formation. *NeuroImage* **242**, 118454 (2021).
48. Roehri, N., Bréchet, L., Seeber, M., Pascual-Leone, A. & Michel, C. M. Phase-amplitude coupling and phase synchronization between medial temporal, frontal and posterior brain regions support episodic autobiographical memory recall. *Brain Topogr.* **35**, 191–206 (2022).
49. Han, C., Shapley, R. & Xing, D. Gamma rhythms in the visual cortex: functions and mechanisms. *Cogn. Neurodyn* **16**, 745–756 (2022).
50. Magazzini, L. & Singh, K. D. Spatial attention modulates visual gamma oscillations across the human ventral stream. *NeuroImage* **166**, 219–229 (2018).
51. Marshall, T. R. et al. Occipital alpha and gamma oscillations support complementary mechanisms for processing stimulus value associations. *J. Cogn. Neurosci.* **30**, 119–129 (2018).
52. Bartoli, E. et al. Temporal dynamics of human frontal and cingulate neural activity during conflict and cognitive control. *Cereb. Cortex* **28**, 3842–3856 (2018).
53. Zhang, J., Xia, J., Zhou, H. & Wang, S. Gamma synchronization between the medial temporal lobe and medial frontal cortex for goal-directed visual attention in humans. *Cell Rep.* **44**, 115905 (2025).
54. Arif, Y. et al. Altered age-related alpha and gamma prefrontal-occipital connectivity serving distinct cognitive interference variants. *NeuroImage* **280**, 120351 (2023).
55. Embury, C. M., Lord, G. H., Drincic, A. T., Desouza, C. V. & Wilson, T. W. Differential impact of glycemic control and comorbid conditions on the neurophysiology underlying task switching in older adults with type 2 diabetes. *Aging* **14**, 4976–4989 (2022).
56. McDonald, K. M. et al. Altered functional connectivity dynamics serving cognitive flexibility in regular cannabis users. *Addict. Biol.* **30**, e70023 (2025).
57. Hald, L. A., Bastiaansen, M. C. M. & Hagoort, P. EEG theta and gamma responses to semantic violations in online sentence processing. *Brain Lang.* **96**, 90–105 (2006).
58. Packard, P. A., Steiger, T. K., Fuentemilla, L. & Bunzeck, N. Neural oscillations and event-related potentials reveal how semantic congruence drives long-term memory in both young and older humans. *Sci. Rep.* **10**, 9116 (2020).
59. Barraza, P., Chavez, M. & Rodríguez, E. Ways of making-sense: local gamma synchronization reveals differences between semantic processing induced by music and language. *Brain Lang.* **152**, 44–49 (2016).
60. Ruzich, E., Crespo-García, M., Dalal, S. S. & Schneidman, J. F. Characterizing hippocampal dynamics with MEG: a systematic review

- and evidence-based guidelines. *Hum. Brain Mapp.* **40**, 1353–1375 (2019).
61. Hutchison, K. A. et al. The semantic priming project. *Behav. Res. Methods* **45**, 1099–1114 (2013).
 62. Brysbaert, M., Warriner, A. B. & Kuperman, V. Concreteness ratings for 40 thousand generally known English word lemmas. *Behav. Res. Methods* **46**, 904–911 (2014).
 63. Taulu, S. & Simola, J. Spatiotemporal signal space separation method for rejecting nearby interference in MEG measurements. *Phys. Med. Biol.* **51**, 1759–1768 (2006).
 64. Gross, J. et al. Good practice for conducting and reporting MEG research. *NeuroImage* **65**, 349–363 (2013).
 65. Uusitalo, M. A. & Ilmoniemi, R. J. Signal-space projection method for separating MEG or EEG into components. *Med. Biol. Eng. Comput.* **35**, 135–140 (1997).
 66. Kovach, C. K. & Gander, P. E. The demodulated band transform. *J. Neurosci. Methods* **261**, 135–154 (2016).
 67. Ernst, M. D. Permutation methods: a basis for exact inference. *Stat. Sci.* **19**, 676–685 (2004).
 68. Maris, E. & Oostenveld, R. Nonparametric statistical testing of EEG- and MEG-data. *J. Neurosci. Methods* **164**, 177–190 (2007).
 69. Sassenhagen, J. & Draschkow, D. Cluster-based permutation tests of MEG/EEG data do not establish significance of effect latency or location. *Psychophysiology* **56**, e13335 (2019).
 70. Gross, J. et al. Dynamic imaging of coherent sources: studying neural interactions in the human brain. *Proc. Natl. Acad. Sci. USA.* **98**, 694–699 (2001).
 71. Van Veen, B. D., Van Drongelen, W., Yuchtman, M. & Suzuki, A. Localization of brain electrical activity via linearly constrained minimum variance spatial filtering. *IEEE Trans. Biomed. Eng.* **44**, 867–880 (1997).
 72. Hillebrand, A., Singh, K. D., Holliday, I. E., Furlong, P. L. & Barnes, G. R. A new approach to neuroimaging with magnetoencephalography. *Hum. Brain Mapp.* **25**, 199–211 (2005).
 73. Wiesman, A. I. & Wilson, T. W. Wilson Attention modulates the gating of primary somatosensory oscillations. *NeuroImage* **211**, 116610 (2020).
 74. *Mixed-Effects Models in S and S-PLUS* (Springer-Verlag, 2000). <https://doi.org/10.1007/b98882>.
 75. Pinheiro, J., Bates, D. & R Core Team. nlme: Linear Nonlinear Mixed Eff. Models 3.1–168, <https://doi.org/10.32614/CRAN.package.nlme> (1999).
 76. Worsley, K. J. et al. A unified statistical approach for determining significant signals in images of cerebral activation. *Hum. Brain Mapp.* **4**, 58–73 (1996).
 77. Poline, J. B., Worsley, K. J., Holmes, A. P., Frackowiak, R. S. & Friston, K. J. Estimating smoothness in statistical parametric maps: variability of p values. *J. Comput. Assist. Tomogr.* **19**, 788–796 (1995).
 78. Barr, D. J., Levy, R., Scheepers, C. & Tily, H. J. Random effects structure for confirmatory hypothesis testing: keep it maximal. *J. Mem. Lang.* **68**, 255–278 (2013).

Acknowledgements

This research was supported by grants R01-MH116782 (Wilson), S10-OD028751 (Wilson), R01-MH118013 (Wilson), R01-DA056223 (Wilson), R01-DA059542 (Wilson), and P20-GM144641 (Wilson, Picci, Taylor, Heinrichs-Graham) from the National Institutes of Health. The funders had no role

in study design, data collection, analysis, decision to publish, or manuscript preparation. We want to thank the participants for volunteering to participate in the study and our staff and local collaborators for contributing to the work.

Author contributions

Conceptualization: T.W.W., E.H.G., G.P.; Data Collection: G.M.G., R.G., H.J.O., A.J.P., J.A.J.; Methodology and Software: Y.A., M.P.R., C.C.C., N.M.P., S.B., P.E.M.-W., E.H.G., H.B., B.K.T., R.K.S.; Formal Analysis: M.C.H., M.P.R., S.M.D., Y.A.; Writing- original draft: M.C.H.; Reviewing and Editing: all authors; Supervision, Resources, and Funding Acquisition: T.W.W. All authors approved the final version for publication and can certify that no other individuals not listed as authors have made substantial contributions to the paper.

Competing interests

The authors declare no competing interests.

Additional information

Supplementary information The online version contains supplementary material available at <https://doi.org/10.1038/s42003-026-09718-4>.

Correspondence and requests for materials should be addressed to Tony W. Wilson.

Peer review information *Communications Biology* thanks the anonymous reviewers for their contribution to the peer review of this work. Primary Handling Editors: Christian Beste and Jasmine Pan. A peer review file is available.

Reprints and permissions information is available at <http://www.nature.com/reprints>

Publisher's note Springer Nature remains neutral with regard to jurisdictional claims in published maps and institutional affiliations.

Open Access This article is licensed under a Creative Commons Attribution-NonCommercial-NoDerivatives 4.0 International License, which permits any non-commercial use, sharing, distribution and reproduction in any medium or format, as long as you give appropriate credit to the original author(s) and the source, provide a link to the Creative Commons licence, and indicate if you modified the licensed material. You do not have permission under this licence to share adapted material derived from this article or parts of it. The images or other third party material in this article are included in the article's Creative Commons licence, unless indicated otherwise in a credit line to the material. If material is not included in the article's Creative Commons licence and your intended use is not permitted by statutory regulation or exceeds the permitted use, you will need to obtain permission directly from the copyright holder. To view a copy of this licence, visit <http://creativecommons.org/licenses/by-nc-nd/4.0/>.

© The Author(s) 2026